Plant Mol Biol
DOI 10.1007/s11103-016-0551-y

The targeting of starch binding domains from starch synthase III to the cell wall alters cell wall composition and properties

Mauricio J. Grisolia[1] · Diego A. Peralta[1] · Hugo A. Valdez[2,3] · Julieta Barchiesi[1] · Diego F. Gomez-Casati[1,2] · María V. Busi[1,2]

Received: 12 May 2016 / Accepted: 13 October 2016

Abstract
Key message **Starch binding domains of starch synthase III from *Arabidopsis thaliana* (SBD123) binds preferentially to cell wall polysaccharides rather than to starch in vitro. Transgenic plants overexpressing SBD123 in the cell wall are larger than wild type. Cell wall components are altered in transgenic plants. Transgenic plants are more susceptible to digestion than wild type and present higher released glucose content. Our results suggest that the transgenic plants have an advantage for the production of bioethanol in terms of saccharification of essential substrates.**

Accession numbers: Starch synthase III, locus name At1g11720; Expansin 8, locus name At2g40610.

Mauricio J. Grisolia and Diego A. Peralta have contributed equally to this work.

Electronic supplementary material The online version of this article (doi:10.1007/s11103-016-0551-y) contains supplementary material, which is available to authorized users.

✉ María V. Busi
busi@cefobi-conicet.gov.ar

[1] Facultad de Ciencias Bioquímicas y Farmacéuticas, Centro de Estudios Fotosintéticos y Bioquímicos - Consejo Nacional de Investigaciones Científicas y Técnicas (CEFOBI - CONICET), Universidad Nacional de Rosario, Rosario, Santa Fe, Argentina

[2] Instituto de Investigaciones Biotecnológicas - Instituto Tecnológico de Chascomús (IIB-INTECH), Universidad Nacional de San Martín, Chascomús, Buenos Aires, Argentina

[3] Present address: Centro de Investigación y Desarrollo en Fermentaciones Industriales (CINDEFI), 50 y 115, 1900 La Plata, Buenos Aires, Argentina

Abstract The plant cell wall, which represents a major source of biomass for biofuel production, is composed of cellulose, hemicelluloses, pectins and lignin. A potential biotechnological target for improving the production of biofuels is the modification of plant cell walls. This modification is achieved via several strategies, including, among others, altering biosynthetic pathways and modifying the associations and structures of various cell wall components. In this study, we modified the cell wall of *A. thaliana* by targeting the starch-binding domains of *A. thaliana* starch synthase III to this structure. The resulting transgenic plants (E8-SDB123) showed an increased biomass, higher levels of both fermentable sugars and hydrolyzed cellulose and altered cell wall properties such as higher laxity and degradability, which are valuable characteristics for the second-generation biofuels industry. The increased biomass and degradability phenotype of E8-SBD123 plants could be explained by the putative cell-wall loosening effect of the *in tandem* starch binding domains. Based on these results, our approach represents a promising biotechnological tool for reducing of biomass recalcitrance and therefore, the need for pretreatments.

Keywords Starch binding domains · Cell wall · Cell extension · Cell wall digestibility · Fermentable sugars

Introduction

The primary cell wall structure of most angiosperms, including *Arabidopsis thaliana*, includes a rigid frame of cellulose microfibrils interacting with soluble xyloglucans that are embedded within the pectin matrix components (Carpita 1996). This scaffold is believed to provide the main

Published online: 21 October 2016

supporting structure of the cell wall and to control many physiological processes, such as wall porosity, charge density alteration and cell growth (Willats et al. 2001). The *Arabidopsis* cell wall also contains several types of structural proteins that may interact both among themselves and with the individual components of the cell wall (Cassab 1998).

In growing cells, this rigid structure must be able to enlarge to the proper size. Cells cannot simply deposit more material to extend the wall, because cells are always compensating for internal turgor pressure (Cosgrove 1993). Thus, a loosening process is required to promote wall flexibility while maintaining structural integrity. Cellular expansion results from the balance between turgor pressure and the mechanical strength of the cell wall. Therefore, the integration of local relaxation and the controlled deposition of new wall materials are required for proper growth coordination. Many proteins, such as expansins, xyloglucan endotransglycosylase and endo-xyloglucan transferase as well as hydroxyl radicals are involved in the wall loosening process. Any attempt to modify cell wall properties (such as lignin/hemicellulose association, surface area and the degree of cellulose crystallinity) (Arantes and Saddler 2010) could directly affect the ability to hydrolyze the associated substrate, avoiding the need to modify the catalytic efficiency of any related enzymatic process.

A carbohydrate-binding module (CBM) is an amino acid sequence within a carbohydrate-active enzyme with a discreet fold that has carbohydrate-binding activity (Cantarel et al. 2009). CBMs have been found in both non-hydrolytic and hydrolytic proteins, several of which are involved in cell wall polysaccharide biosynthesis and degradation. These proteins exhibit a modular molecular structure comprising one catalytic domain and one or more CBMs, which are normally linked by unstructured sequences. CBMs may function via three possible mechanisms: a substrate-catalytic domain approach; protein–protein interactions to create a scaffold; or non-hydrolytic substrate disruption (Shoseyov et al. 2006). Although CBMs generally bind selectively to their substrates, some can bind to other polysaccharides with higher affinity than to their natural substrate (Bolam et al. 1998).

CBMs can facilitate cellulose hydrolysis in vitro through a disruptive mechanism. Specifically, the addition of CBMs from bacteria and fungi facilitates cellulose hydrolysis by physically disrupting the structure of the cellulosic fibrous network, which releases small particles without exhibiting any detectable hydrolytic activity (Abbott and Boraston 2012; Sato et al. 2010; Teeri et al. 1992). However, there are few reports of the overexpression of CBMs in plants. Such CBMs are contained in plant cell wall metabolism-related enzymes (Levy et al. 2002; Nardi et al. 2015; Obembe et al. 2007; Shoseyov et al. 2001, 2006).

Starch binding domains (SBDs) are distinct sequence-structural modules of CBMs that bind to starch. These domains have gained the evolutionary advantage of enabling CBMs to break the structure of the substrate more efficiently due to the presence of two polysaccharide-binding sites (Southall et al. 1999; Tormo et al. 1996). To date, there are no reports describing the expression of SBDs in plant structures other than chloroplasts.

Starch is made up of two types of glucan homopolymers, amylose and amylopectin (Buleon et al. 1998), and is produced by the coordinated actions of a set of enzymes including ADPGlc pyrophosphorylase (ADPGlc PPase), starch synthase (SS), starch branching enzyme (SBE) and starch debranching enzyme (DBE) (Ball and Morell 2003; Busi et al. 2014; James et al. 2003; Tetlow et al. 2004; Zhang et al. 2008). Each SS has a specific function that it performs in a specific location, and therefore, these enzymes are not redundant: GBSS (granule bound starch synthase) is nearly exclusively granule-bound, whereas the four other classes are distributed between the stroma and granule (SSI, SSII) or are located entirely in the stroma (SSIII, SSIV) (Busi et al. 2014; Denyer et al. 1993; Zhang et al. 2008).

Starch synthase III (SSIII, At1g11720) from *A. thaliana* possesses a typical modular structure comprising an N-terminal transit peptide for chloroplast localization, followed by three repeated SBDs belonging to the CBM53 family (http://www.cazy.org/CBM53.html), named D1, D2 and D3, residues 22–591 and a C-terminal catalytic domain (residues 592–1025) (Valdez et al. 2008, 2011). This C-terminal catalytic domain is similar to that found in bacterial glycogen synthases, however, these enzymes lack SBDs (Busi et al. 2008; Gomez-Casati et al. 2013; Palopoli et al. 2006; Valdez et al. 2008). We previously reported the binding of the different SBDs to raw starch and its individual components, amylose or amylopectin. Our results show that the D1 domain is essential for providing the enzyme with a higher affinity for the amylose fraction (Valdez et al. 2011). This preference of SBD123 for the linear fraction of starch (Valdez et al. 2011), the binding promiscuity of SBDs and the existence of two polysaccharide binding sites, which was predicted in silico and experimentally, together with the ability of SBD to act *in trans* with the catalytic domain of AtSSIII (Wayllace et al. 2010), have led us to postulate that these domains could bind to polysaccharides other than their natural substrates, such as cell wall polysaccharides.

In this study, we show that the N-terminal region of *A. thaliana* SSIII (SBD123) can bind to cell wall polysaccharides. Furthermore, this domain was successfully directed to the cell walls of *A. thaliana* plants, which led to a marked increase in biomass degradability, as well as the increased release of glucose units. These results suggest that these SBDs could be used as a potential biotechnological tool for the modification of plant cell walls. This approach could be utilized to solve specific problems in the biofuel and livestock feed industries.

Materials and methods

Plant material and growth conditions

Wild-type *A. thaliana* (var. Columbia Col-0) and two independent transgenic lines, E8-SBD123.1 and E8-SBD123.2, were used in this study. All plants were grown in soil in a greenhouse at 25 °C under fluorescent lamps (Grolux, Sylvania, Danvers, MA, USA and Cool White, Philips, Amsterdam, The Netherlands), with an intensity of 150 µmol m^{-2} s^{-1} and a 16 h light/8 h dark photoperiod. The seeds were treated for 3 days at 4 °C. After 2 weeks, transgenic plants were selected on 5 mg/L ammonium glufosinate Basta™ (Bayer CropScience AG, Germany).

Molecular cloning of *SBD123* from *A. thaliana*

Total RNA was isolated using Tri reagent (Sigma-Aldrich, St. Louis, MO) and used as a template for cDNA synthesis using oligo(dT) primer and the MVLV RT-PCR system (USB Corp., Cleveland, OH). The cDNA for SSIII (At1g11720) was amplified by PCR using *Pfu* polymerase (Promega, Madison, WI) and the following primers: 123up, AGAGCATATGAGTGCTCAGAAAA; SBDdo, CTGCTCGAGTGGTTCCTTTGAAAT. The resulting PCR product was digested with restriction enzymes NdeI and XhoI (Promega, Madison, WI) and cloned in the pET32c vector (Novagen Inc., Madison, WI). XL1Blue *E. coli* cells were transformed, and positive clones were verified by DNA sequencing.

Expression and purification of recombinant SBD123 and mutated SBD123 proteins

Recombinant SBD123 and the mutated proteins SBD123W340A, SBD123W366A and SBD123Y394A were used for the binding assays (Valdez et al. 2008, 2011). For expression of these proteins, the pVAL123 vector (and its mutated forms) were transformed into BL21-CodonPlus (DE3)-RIL *E. coli* competent cells (Valdez et al. 2011). The cells were grown at 37 °C for 4 h, followed by the addition of 0.5 mM IPTG and incubation at 28 °C for 4 h. The cells were harvested by centrifugation (4000×*g*, 10 min, 4 °C), and the pellet was washed and suspended in 20 mM Tris-HCl (pH 8). The cells were disrupted using an ultrasonicator (VCX130, Sonics and Materials Inc.), centrifuged (12,000×*g*, 15 min, 4 °C) and filtered through a 0.2 µm cellulose acetate membrane. Purification of all recombinant proteins (native and mutated) was performed using a HiTrap chelating HP column (Amersham Biosciences) equilibrated with binding buffer [20 mM Tris-HCl (pH 8), 0.3 M NaCl, 1 mM β-mercaptoethanol and 20 mM imidazole]. The column was washed with 10–15 volumes of binding buffer, and each protein was eluted using a linear gradient of binding buffer and elution buffer [20 mM Tris-HCl (pH 8), 0.3 M NaCl, 1 mM β-mercaptoethanol, and 0–500 mM imidazole]. The presence of the recombinant proteins was monitored by SDS-PAGE and immunoblotting using a-His antibody (Santa Cruz Biotechnology, Dallas, TX). The purified protein fractions were pooled and concentrated to >1 mg/ml using Centriplus-10 and Centriprep-10 concentrators (Millipore Corp., Billerica, MA). The concentrated proteins were desalted and used to determine enzyme activity or stored at −20 °C until use.

Polysaccharide binding assay

Adsorption of SBDs to starch and cell wall polysaccharides was determined as described previously with minor modifications (Rodriguez-Sanoja et al. 2005). The polysaccharides used were starch from wheat (Fluka #85649), pectin from apple (Sigma, #76282), xylan from beechwood (Sigma, #4252) and cellulose microcrystalline (Biopack, #171307).

Purified recombinant SBD123 protein (final concentration of 0–80 µM) was added to a prewashed polysaccharide suspension (10 %, w/v) in 100 mM citrate-phosphate buffer (pH 5) to a final volume of 60 µL. Each mixture was incubated at 4 °C for at least 1 h with gentle shaking (10 rpm) and centrifuged at 12,000×*g* for 5 min at 4 °C. The amount of bound protein was determined by subtracting the amount of protein in the supernatant from the total amount of protein added to the mixture. The protein concentration was determined by measuring the absorbance at 280 nm. Polysaccharide absorption was subtracted for each condition (control), and BSA was used as a negative binding control. The adsorption constant (K_{ad}, in ml/g of polysaccharide) was determined from the slope as previously reported (Rodriguez-Sanoja et al. 2005) in three biological replicates and then compared statistically as described in the "Statistical analysis" section.

Vector construction, transformation and selection of plants

A chimeric construct containing the sequence of the signal peptide of *A. thaliana* expansin 8 (At2g40610) fused to the sequence coding for the three SBDs (SBD123) from AtSSIII (At1g11720, residues 181 to 644) was cloned into the pDONR221™ vector and recombined into plant expression vector pCTAPi298 (Rohila et al. 2004) using Gateway® technology (Life Technologies,, Carlsbad, CA, USA). The chimeric construct is expressed under the 35S CaMV constitutive promoter from pCTAPi298. This construct was used to transform *A. thaliana* Col-0 plants by the floral dip method using *Agrobacterium tumefaciens* (Clough 1998). Transgenic plants were selected on the commercial

herbicide Basta™ (Bayer CropScience AG, Germany). The presence of the transgene was confirmed by PCR of genomic DNA with the following primers: GtwUpEx8At, GGGGACAAGTTTGTACAAAAAAGCAGGCTAAATGTACACTCCATCATACTTA and D2 Down Xho AAACTCGAGTCTTTCCTTAGTTTCAGC.

Isolation of RNA and qRT-PCR analysis

Total RNA was extracted from roots, stems, rosette leaves and flowers at 28 days after germination (stage 5) (Boyes et al. 2001) using the SV Total RNA Isolation System (Promega, Madison, WI, USA). Complementary DNA was synthesized using random hexamers and the M-MLV reverse transcriptase protocol (Promega, Madison, WI, USA). Quantitative reverse-transcription PCR (qRT-PCR) was carried out in a MiniOPTICON2 apparatus (BioRad, Hercules, CA, USA) using the intercalation dye SYBR Green I (Invitrogen, Carlsbad, CA, USA) as a fluorescent reporter and Go Taq polymerase (Promega, Madison, WI, USA). Primers suitable for the specific amplification of the transgene were designed using PrimerBlast software (Ye et al. 2012) (E8-SBD123Fw: CCTCCAAGGAACTCATGGAGACG and E8-SBD123Rv: CGGGTTCGTTATTCAGAGTCGACA). The amplification conditions were as follow: 2 min denaturation at 94 °C; 40 cycles at 94 °C for 10 s, 63 °C for 15 s and 72 °C for 20 s, followed by 10 min extension at 72 °C. Three experimental replicates were performed for each biological replicate. Melting curves were determined by measuring the decrease in fluorescence with increasing temperature (from 65 to 98 °C). PCR products were run on a 2% (w/v) agarose gel to confirm the sizes of the amplification products and to verify the presence of a unique PCR product. Relative transcript levels were calculated as the ratio of the transcript abundance of the studied gene to the transcript abundance of *β-ACT* [At3g18780] (ACT2F1: TGCTGGAATCCACGAGACAACCTA and ACT2R1: TGCTGAGGGAAGCAAGAATGGAAC).

Immunohistochemistry and subcellular localization by confocal microscopy

Histological sections of *A. thaliana* Col-0, E8-SBD123.1 and E8-SBD123.2 leaves were subjected to immunohistochemical analysis by incubating them with primary antibody directed against SBD2 followed by a-rabbit IgG TRITC-conjugated antibody (Sigma, #T5268). The cell walls were stained with calcofluor (Sigma, #F3543). The co-localization of SBD123 with the cell wall was analyzed and visualized by confocal microscopy under the 40× objective. The confocal microscope was a Nikon C1Plus attached to a Nikon Eclipse TE2000-E2 inverted microscope. TRITC and calcofluor were excited at 440 and 557 nm, respectively, and the emission was collected at 520 for TRITC and 576 nm for calcofluor. The experiment was repeated at least three times. The whole displayed image was adjusted for brightness and contrast solely to show the details using EZC1 software.

Rosette expansion curve analysis

Construction of the rosette expansion curve was performed as described in Rymen et al. (2010) with some modifications. The plants were grown in soil as indicated above ("Plant material and growth conditions"), and digital images were acquired. The images were processed with ImageJ software (Abramoff et al. 2004), and total rosette areas were determined. Finally, these parameters were plotted against time, and two-way ANOVA tests were performed, defining two factors with different levels: plant type (Col-0, E8-SBD123.1 and E8-SBD123.2) and time (each day as a different level).

Measurement of growth phenotype

At least ten plants at stage 5 were harvested for fresh weight measurements and subsequently dried at 60 °C to constant weight for dry weight measurements. The parameter dry matter (DM) was calculated as dry weight/fresh weight (kg kg^{-1}). Quality Index (QI), which was adapted for *A. thaliana* from Ritchie et al. (1984) as a measure of globally desirable phenotype, was calculated as $QI = \{[RDW + SDW]/[SL/(RD/10)]\} + [SFW/RFW]$, where RDW is root dry weight, SDW is stem dry weight, SL is stem length, RD is root diameter, SFW is stem fresh weight and RFW is root fresh weight. Stem elongation rate (SER) was determined as described in Weigel and Glazebrook (2002). For root elongation rate, plants were grown in Murashige–Skoog (MS) agar medium and the root length was recorded for approximately 15 days (Weigel and Glazebrook 2002). Flowering time was determined using several parameters, such as the number of rosette leaves (Koornneef et al. 1991), the appearance of the shoot apex, the appearance of the first flower bud and stem length (Weigel and Glazebrook 2002). All parameters were determined individually for each plant line and compared statistically as described in the "Statistical analysis" section.

Microscopic observations

Arabidopsis thaliana stems were prepared for transmission electron microscopy (TEM) by fixing overnight in 2.5% glutaraldehyde in phosphate buffer (0.1 M, pH 7.4), followed by post-fixing for 1 h 30 min in 1% (p/v) osmium tetroxide in phosphate buffer (0.1 M, pH 7.4). The samples were then stained in 5% (p/v) uranyl acetate in water, dehydrated in a graded alcohol series (50, 70, 96, 2× 100%),

followed by acetone (at least 15 min per step) and embedded in Spurr's resin. Thin sections were cut with a diamond knife and viewed under a Zeiss 109T electron microscope (Carl Zeiss Microscopy GmbH, Jena, Germany) with a GATAN digital camera (GATAN Inc., Warrendale, PA, USA). Cell wall thickness was determined in stems using the ImageJ program (Abramoff et al. 2004).

Cell area was determined in stem medullar parenchymal tissue and leaves by optical microscopy. For this, both tissues were fixed with FAA and cleared with chloral hydrate solution as described previously (Horiguchi et al. 2005; Rodriguez et al. 2010). Palisade leaf cells were observed one-fourth of the way down/up from the tip/bottom and halfway between the leaf margin and the mid-vein, avoiding highly optically disturbed zones due to the presence of vascular tissue (Rymen et al. 2010). Images were obtained by differential interference contrast (DIC) microscopy using an Olympus BH-2 microscope (Olympus Corporation, Shinjuku, Tokyo, Japan) and a Nikon digital Sight DS-Fi1 digital camera (Nikon Corporation, Tokyo, Japan).

Cell wall extraction and analysis

Cell wall polysaccharides were obtained as alcohol insoluble residue (AIR) according to d'Amour et al. (1993) and Vicente et al. (2005) with some modifications. Stem tissue (2 g) was homogenized in 8 ml of ethanol and boiled for 30 min. The homogenate was filtered, the residue was washed three times with 10 ml of ethanol and the solvent was evaporated under a vacuum at 20 °C. The resulting dried residue (AIR) was used to prepare different cell wall fractions. All subsequent experiments were performed with three biological replicates and at least two experimental replicates.

Pectin and hemicelluloses quantification

AIR samples (100 mg) were homogenized in 100 ml of water (overnight; 20 °C with agitation), filtered and washed three times with 10 ml of deionized water (Water soluble pectins). The residue was resuspended in 100 ml of EDTA-acetate buffer (0.05 M sodium acetate; 0.04 M EDTA) for 4 h at 20 °C, filtered and washed three times with 10 ml of the buffer (EDTA soluble pectins). The residue was then resuspended in 100 ml of 0.05 M HCl (1 h; 100 °C), cooled, filtered and washed three times with 10 ml of 0.05 M HCl (HCl soluble pectins). The washings were pooled and stored at −20 °C. The remaining residue was used for hemicellulose quantification: the material was stirred with 100 ml of 4 M NaOH (8 h; 20 °C), filtered and washed three times with 5 ml of 4 M NaOH (hemicellulose fraction). All fractions were hydrolyzed via a final incubation in 66 % (v/v) H_2SO_4 (60 min; 100 °C), and glucose content was estimated using the anthrone method (d'Amour et al. 1993; Vicente et al. 2005). The amount of uronic acid released after pectin hydrolysis was measured by the *m*-hydroxydiphenyl method (Blumenkrantz and Asboe-Hansen 1973) using galacturonic acid (GA) as a standard.

Lignins quantification

Acetyl bromide lignin determination was performed as described previously (Hatfield et al. 1999; Iiyama and Wallis 1988) with some modifications. First, 5 mg of the alcohol insoluble residue was treated with 25 % acetyl bromide (w/w) in glacial acetic acid for 30 min at 70 °C. The samples were then neutralized with 2 N NaOH and glacial HAc in sufficient quantity for a final volume of 100 ml. Lignin quantification was carried out by measuring absorbance at 290 nm.

Cell wall hydrolysis and metabolite determination

Sample preparation and cell wall extraction were carried out as described above (see "Cell wall extraction and analysis" section). Cell wall hydrolysis was carried out according to Minic et al. (2009). For metabolite GC/MS profiling, 60 µl of ribitol (0.3 mg/ml) and 750 µl of chloroform were added to the sample prior to centrifugation at 2200×*g* for 15 min, and derivation was performed as described by Lisec et al. (2006).

For analysis, four biological replicates per treatment with a second group of technical replicates were utilized (eight total data points). GC–MS analysis was performed using an autosystem XL Gas Chromatograph and a Turbo Mass Spectrometer (Perkin Elmer). One microliter split injection (split ratio 1:40) was injected at 280 °C. The capillary column used was a VF-5 ms column (Varian, Darmstadt, Germany) with helium as the carrier gas with constant flow at 1 ml/min. The temperature program was 5 min at 70 °C, 5 min ramp-up to 310 °C and final heating for 2 min at 310 °C. The transfer line to the MS was set to 280 °C. Spectra were monitored in the mass range m/z = 70–600. Tuning and all other settings were according to the manufacturer's recommendations. Chromatograms were acquired with TurboMass 4.1 software (Perkin Elmer). The NIST98mass spectral search program (National Institute of Standards and Technology, Gaithersburg, MD, USA) was the software platform utilized. The MS and retention time index were compared with the values in the Golm Metabolome Database (Kopka et al. 2005). MS matching was manually supervised, and matches with thresholds of match >650 (with maximum match equal to 1000) and retention index deviation <1.0 % were accepted. Peak heights were normalized using the amount of the sample fresh weight and ribitol for internal standardization. Relative metabolite contents were determined, and

statistical analyses were performed using one-way ANOVA (see Statistical analysis).

Enzymatic fermentable sugars determination

Plants were grown under a long-day cycle for 28 days and harvested at different times of the day: at end of the night (8 h), at midday (16 h) and at the beginning of the night (24 h). Total leaf extracts (100 mg) were deproteinized using 1 M perchloric acid, and plant extracts were dissolved in 300 mM triethanolamine buffer (pH 7.5), filtered, and subjected to enzymatic treatment as described in (Bergmeyer 2012) to determine glucose, fructose and galactose contents, following the formation of NADPH at 340 nm.

Protoplast isolation

Protoplast isolation was performed using leaves of stage 5 plants as starting material as described in Yoo et al. (2007). Digestion of the cell wall occurred over a fixed time (3 h) but with different amounts of cellulase/macerozyme, generating different conditions: 0.5 [0.5 % (w/v)/0.15 % (w/v)]; 1 [1 % (w/v)/0.3 % (w/v)]; 1.5 [1.5 % (w/v)/0.45 % (w/v)] and 2 [2 % (w/v)/0.6 % (w/v)]. Statistical analysis was carried out as described below ("Statistical analysis").

In vitro dry matter digestibility assay

The in vitro dry matter digestibility (DMD) assay was performed as described in Tilley and Terry (1963) with slight modifications. Oven-dried stem samples (0.2 g) from Col-0, E8-SBD123.1 and E8-SBD123.2 were incubated with strained rumen liquor at 40 °C in the dark for 48 h, with four daily agitations. The samples were then centrifuged for 15 min. at 1800×*g* and the pellet was treated with 50 ml chymosin solution (1 g/ml in 0.075 N HCl) at 40 °C for 48 h with occasional shaking. The insoluble residues were washed with water and dried at 100 °C to constant weight. The dry weight of "blank" tubes (which represented undigested food particles and microorganisms derived from the rumen liquor) was subtracted, and the DMD was calculated as the weight of digestible material per 100 g of stem dry matter.

Statistical analysis

The experiments were performed according to a completely randomized design factorial design in which the main factor was plant type (Col-0, E8-SBD123.1 and E8-SBD123.2) unless otherwise noted. Normality assumption was corroborated with Shapiro–Wilk's test, and equal variance was corroborated with Levene's test. When the normality assumption was not fulfilled, a non-parametric ANOVA (Kruskal–Wallis) was used. To isolate the group or groups that differed from the others, a parametric (Tukey) or a non-parametric (Dunn) multiple comparison test was used. Each test was performed at a significance level of 0.05.

Results

SBD123 binds preferentially to cell wall polysaccharides rather than to starch

We previously demonstrated that SBDs cooperatively bind to storage polysaccharides such as starch, amylopectin and (more markedly) amylose, suggesting a preference for linear polysaccharides (Valdez et al. 2008, 2011). To evaluate the adsorption of SBDs to structural polysaccharides, we investigated the ability of SBD recombinant protein to bind to different polysaccharide components of the plant cell wall by performing a binding assay. As shown in Fig. 1, SBD123 could bind to xylan and pectins with a twofold higher affinity than to starch, while the K_{ad} for cellulose was 2.4-fold higher than that for starch. Thus, SBD123 could bind to the three polysaccharide cell wall components tested, which reflects the promiscuity of these domains, since SBD123 not only binds to its natural substrate, but it also binds to the other carbohydrates with higher affinity. BSA, which was used as control, did not significantly bind to any polysaccharide tested (not shown), suggesting that the binding ability of SBD123 is specific. In addition, we evaluated if

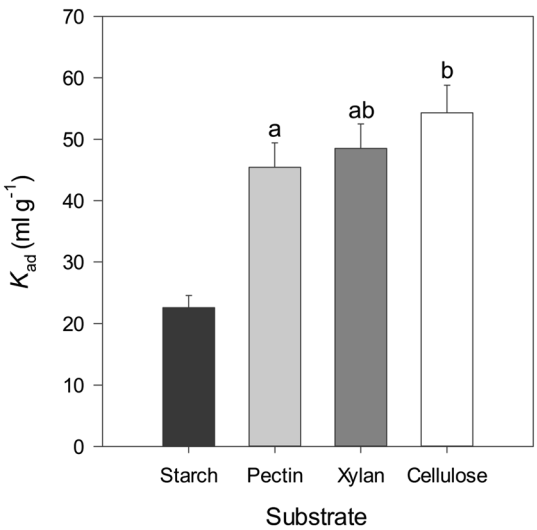

Fig. 1 SBD123 binds to starch and cell wall polysaccharides in vitro. K_{ad} values for the adsorption of recombinant SBD123 to starch (*black*), pectin (*light gray*), xylan (*gray*) and cellulose (*white*). The data shown are the mean ± SD of three biological replicates. *Lowercase letters* (*a* and *b*) indicate group or groups that differ from the others using a multiple comparison procedure (Tukey) after statistical analysis with an $\alpha = 0.05$

the amino acid residues involved in starch binding (W340, W366 and Y394), are also responsible to the binding to plant cell wall polysaccharides (Valdez et al. 2011). Results confirm the participation of these amino acid residues in the adsorption to the substrates, being the Y394 the most relevant (see Supplementary Table 1).

SBD123 is directed to the *Arabidopsis thaliana* cell wall

A chimeric construct harboring the gene encoding the N-terminal region of *A. thaliana* AtSSIII (At1g11720) containing the three SBDs (SBD123) fused with the signal peptide of *A. thaliana* expansin 8 (At2g40610) was cloned into the vector pDONR221™ and recombined to pCTAPi298 (Rohila et al. 2004) as described in the "Materials and methods" section.

After plant transformation and selection, two independent transgenic lines, E8-SBD123.1 and E8-SBD123.2, were isolated at 21 days post-germination. Transgene expression analysis (qRT-PCR) was conducted using specific primers (designed to span the transit peptide and SBD1 sequence): E8-SBD123Fw: CCTCCAAGGAACTCATGGAGACG and E8-SBD123Rv: CGGGTTCGTTATTCAGAGTCGACA, with an amplification product of 155 bp. Several organs (roots, stems, leaves and flowers) of these lines and Col-0 plants were tested, which showed that the transgene was expressed correctly in both transgenic lines and that it was not present in Col-0 plants (Supplementary Fig. 1).

To verify the correct localization of SBD123 in the transgenic plants, we carried out confocal microscopy and immunohistochemistry assays in the wild-type and transgenic lines (Fig. 2). A highly antigenic custom-made a-SBD2 was used as the primary antibody and a-rabbit IgG-TRITC conjugate was used as the secondary antibody (yellow). Cell walls were stained with calcofluor (blue). The white color in the merged images (blue + yellow) suggests the correct expression and localization of SBD123 in the cell walls of transgenic plants (Fig. 2). The a-SBD2 antibody is capable of binding endogenous SSIII located in the chloroplast. As shown in Fig. 2, TRITC fluorescence was detected in these organelles in both Col-0 and the transgenic lines. However, this fluorescence did not co-localize with cell wall calcofluor fluorescence in the Col-0 lines.

E8-SBD123 plants are larger than wild type

Growth is a key parameter used to evaluate the relevance of a specific genotype in applied crop sciences (Beemster and Baskin 1998). In the current study, the visual inspection of transgenic plants suggested that the E8-SBD123 lines grew normally, although they were noticeably larger than wild-type plants (Fig. 3a). In addition, both transgenic lines exhibited the same growth behavior compared with Col-0 plants (Supplementary Fig. 2).

We detected an approximately 1.76-fold increase in both plant fresh and dry weights in lines E8-SBD123.1 and E8-SBD123.2 compared with Col-0 plants (Table 1). To determine if there was a significant surge in growth rate in the plants, we measured their rosette areas daily (see "Materials and methods"). A shown in Fig. 3b, we detected a significant increase in rosette area beginning on day 16 after germination. Stage 1 growth in *A. thaliana* (Boyes et al. 2001) is thought to be mainly driven by cellular proliferation, whereas beginning at stage 3, growth is directed by cellular expansion (Donnelly et al. 1999). Therefore, we investigated whether there was a difference in cellular expansion-directed growth between the plant types.

Although growth assessment can be a relatively direct process, the application of a combination of two or more morphological measurements (morphological index) can be used to describe an abstract state of a seedling, such as the relative importance of a particular factor to field performance (Duryea 1985). For example, a modified version of the Dickson's quality index (QI) (Ritchie 1984) summarizes the general phenotypic status of a plant, establishing a relationship between stem and root dry weight, stem and root fresh weight, root diameter and stem length (see "Materials and methods" section). This parameter was significantly higher in E8-SBD123.1 (12.45) and E8-SBD123.2 (11.66) than in Col-0 (6.52), which parallels the visually observed differences between these lines (see Table 1).

The shift from vegetative to reproductive growth is an important event in a plant's lifecycle. The flowering time parameter, which is modulated by both environmental and endogenous factors, is a good indicator of plant stress state. In plants grown under normal conditions and a long-day regime, *A. thaliana* ecotype Col-0 flowers appear within 3–4 weeks after sowing (Boyes et al. 2001; Koornneef et al. 1991). Once we confirmed that Col-0 and both transgenic lines germinated at the same time, we proceeded to evaluate the flowering time using several approaches, such as counting the number of rosette leaves (Koornneef et al. 1991) and observing the occurrence of the shoot apex, the appearance of the first flower bud and stem length (Weigel and Glazebrook 2002) (Supplementary Fig. 3). We found that flowering occurred approximately 2 days earlier in the E8-SBD123 lines than in Col-0 plants, suggesting that the transgenic plants undergo an early entrance into the reproductive stage.

Finally, we found that the stem and root elongation rates were significantly increased in both transgenic lines compared to Col-0. SER increased approximately 1.9-fold and 1.5-fold in E8-SBD123.1 and E8-SBD123.2, respectively, while RER increased 1.5-fold in E8-SBD123.1 and 1.6-fold in E8-SBD123.2 compared to wild type (Table 1).

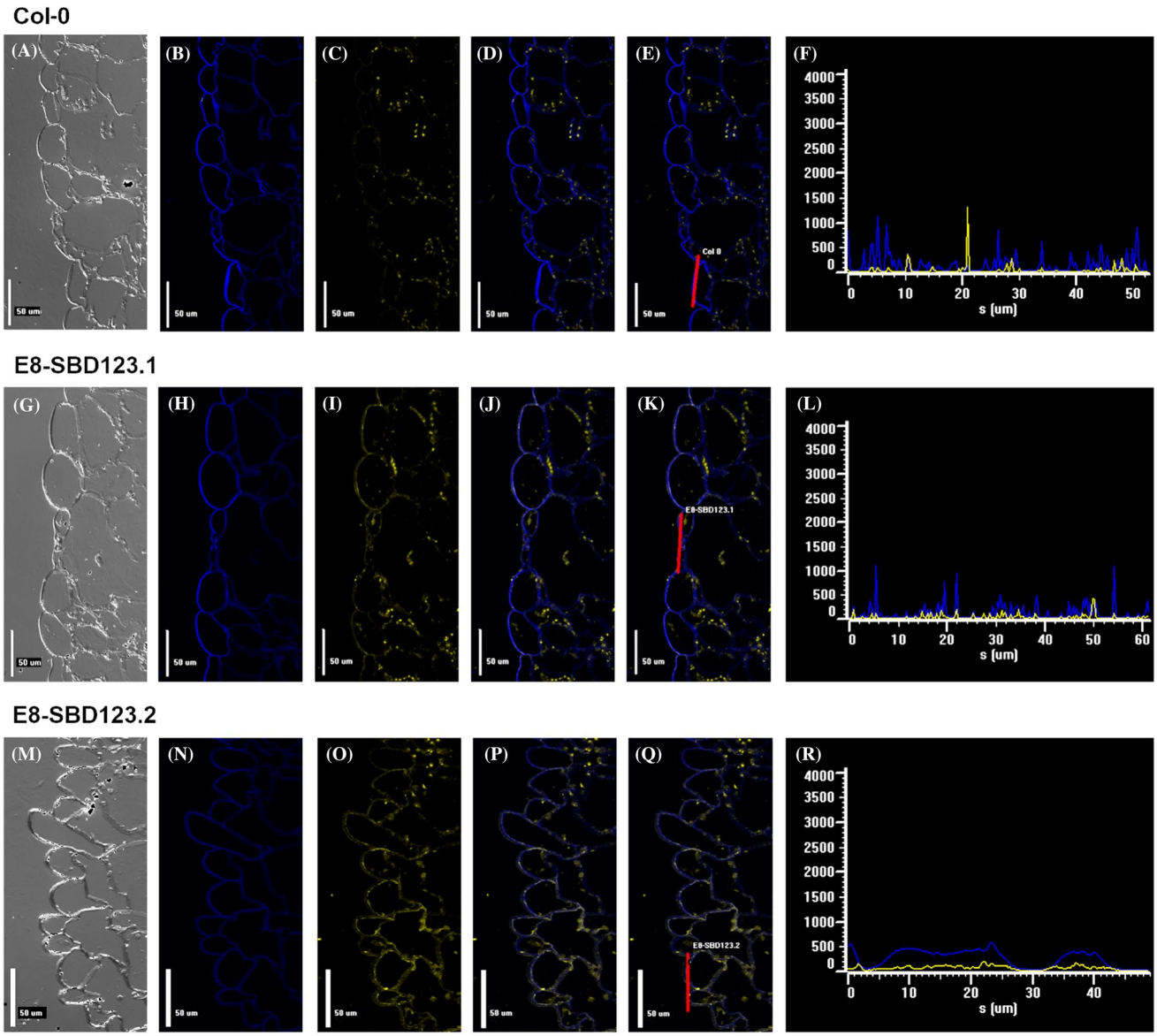

Fig. 2 Subcellular localization of SBD123 in *A. thaliana* Col-0 and E8-SBD123 lines. Confocal laser-scanning micrographs showing the localization of SBD123 in *Arabidopsis* leaves from Col-0 (**a**–**e**), E8-SBD123.1 (**g**–**k**) and E8-SBD123.2 (**m**–**q**). The cell walls were stained with calcofluor (*blue*), and SBD123 was immunodetected using anti-SBD2 followed by a-rabbit IgG TRITC conjugated (*yellow*). *Panels* **d, j** and **p** show the signal overlap, and *panels* **f, l** and **r** show the fluorescence emission intensity profile graph for each channel of the spectra of emission (along the *indicated lines* in *panels* **e, k** and **q**). Whole displayed images were adjusted for brightness and contrast solely to show details using EZC1 software. The experiments were repeated three times with similar results

Cellular expansion leads to biomass production

Leaf palisade parenchymal tissue is highly organized, with vertically elongated cells and few intracellular spaces (Rymen et al. 2010). Therefore, fully grown foliar limb area is thought to be equivalent to the mean transverse cellular area multiplied by the mean cell number (Horiguchi et al. 2005). We assayed these parameters in leaves 1–2 of stage 5 plants, whose growth had completely stopped (see Table 2), finding an approximately 1.4-fold increase in the leaf areas of both E8-SBD123 lines, which is completely explained by the 1.4-fold increase in cellular area in both transgenic lines. There was no difference in mean cell number between the wild-type and transgenic lines.

Since stem medullar parenchymal tissue is considered to be well defined, we also evaluated the mean cellular area in this tissue (Table 2), finding a 1.3-fold increase in this area in both E8-SBD123.1 and E8-SBD123.2 cells. We also evaluated primary cell wall thickness in stems from growing plants (stage 3) through TEM (Turner Somerville

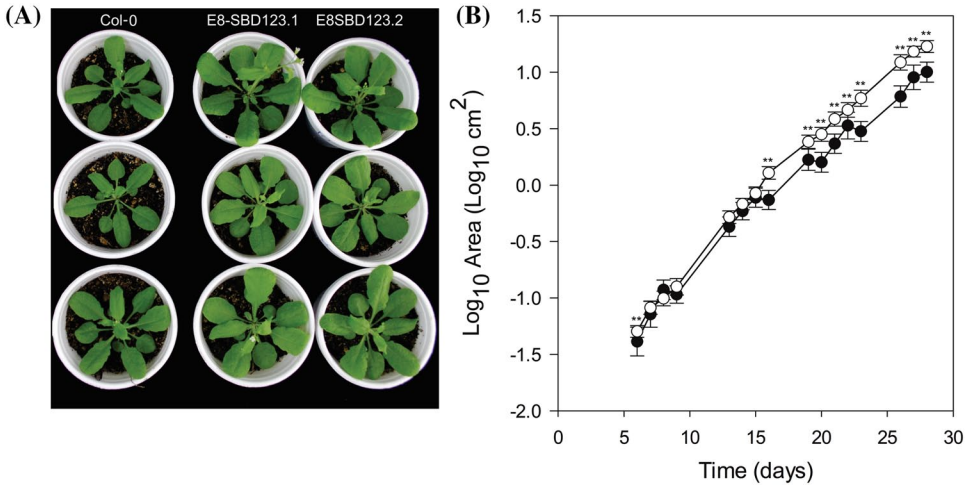

Fig. 3 Growth phenotypes of Col-0 and E8-SBD123 plants. **a** Transgenic plants show an increased-size phenotype through 28 days after germination. E8-SBD123.1 and E8-SBD123.2 are two independent lines. **b** Growth analysis showing the logarithmic transformation of rosette area through time for plant line E8-SBD123.1 (*open circle*) in contrast with Col-0 plants (*closed circle*). **Significant difference at $p < 0.01$

Table 1 Growth parameters of Col-0 and E8-SBD123 lines

Parameter	Col-0	SD	E8-SBD123.1	SD	E8-SBD123.2	SD	$p < 0.05$
Quality index	6.524^a	1.734	12.447^b	3.444	11.662^b	3.573	Yes*
Total fresh weight (g)	1.000^a	0.379	1.617^b	0.383	1.786^b	0.165	Yes**
Total dry weight (g)	0.073^a	0.018	0.125^b	0.035	0.119^b	0.025	Yes*
Root elongation rate (cm day^{-1})	0.473^a	0.194	0.702^b	0.164	0.739^b	0.186	Yes*
Stem elongation rate (mm/day)	12.599^a	3.815	24.030^b	8.169	24.112^b	3.993	Yes*

All comparisons were conducted using a parametric ANOVA with an $\alpha = 0.05$

Lowercase letters (a and b) indicate the group or groups that differ from the others using a multiple comparison procedure. Significant difference at *$p < 0.05$; **$p < 0.01$

Table 2 Mean cell area in leaves and stems; leaf area and cell number in stems in *Arabidopsis thaliana* Col-0 and E8-SDB123 lines

Organ	Line	Cell area (mm^2)			Leaf area (mm^2)			Cell No.		
		Mean	SD	p	Mean	SD	p (vs. Col-0)	Mean	SD	p (vs. Col-0)
Leaf	Col-0	0.00213^a	–	$<0.001^\dagger$	36.595^a	4.242	0.023	16,729	*	$0.629^\dagger$
	E8-SBD123.1	0.00284^b	–		50.288^b	0.578		17,011	*	
	E8-SBD123.2	0.00294^b	–		51.376^b	7.957		15,342	*	
Stem	Col-0	0.00136	–	$0.002^\dagger$	–	–	–	–	–	–
	E8-SBD123.1	0.00174	–		–	–		–	–	
	E8-SBD123.2	0.00175	–							

All comparisons were conducted using an ANOVA with an $\alpha = 0.05$

†Indicates the use of a non-parametric ANOVA (Kruskal–Wallis). Lowercase letters (a and b) indicate the group or groups that differ from the others using a multiple comparison procedure (Tukey)

CR: Collapsed xylem phenotype of Arabidopsis identifies mutants deficient in cellulose deposition in the secondary cell wall 1997) (Supplementary Fig. 4), finding a 27% reduction in cell wall thickness in both E8-SBD123 lines compared to wild type. These results suggest that the change in plant biomass in the transgenic lines is mainly due to an increase in cellular expansion rather than cellular proliferation.

Cell wall components are altered in transgenic plants

Cell walls undergo dynamic changes during plant cell expansion in order to acquire the mechanical properties required for cell growth. Therefore, we performed a detailed analysis of stem cell wall components of Col-0 and SBD123-expressing plants using an enzymatic approach (d'Amour et al. 1993). The proportions of the different cell wall

fractions were determined using 100 mg of AIR (Alcohol insoluble residue) as starting material (Fig. 4). The cellulose and lignin contents of both transgenic lines and wild-type cell walls were similar. However, we detected a 1.3-fold increase in the pectin content and a 1.5-fold increase in the hemicellulose content in the cell walls of both transgenic lines compared to Col-0.

We conducted metabolomics (GC-MS) studies of leaf cell wall hydrolysates (Hoebler et al. 1989) to investigate whether these differences led to differences in the sugar compositions of cell wall polysaccharides in the transgenic lines (Minic et al. 2009). The results show an increase in the contents of both glucose (1.9-fold for E8-SBD123.1 and E8-SBD123.2) and galactose (2.0-fold and 2.3-fold for E8-SBD123.1 and E8-SBD123.2, respectively), a decrease in xylose content (approximately 0.5-fold for E8-SBD123.1 and E8-SBD123.2) and a decrease in the content of the non-resolved pentose pool (approximately 0.6-fold for both E8-SBD123.1 and E8-SBD123.2) in the transgenic plants compared wild type (see Fig. 4).

The percentage of glucose released by the transgenic plants compared to Col-0 was quantified using the equation reported by Larran et al. (2015). While this value was close to 85% (85.6 ± 4.6) in wild-type plants, the values for both transgenic lines were greater than 97% (E8-SBD123.1: 97.2 ± 2.4; E8-SBD123.2: 98.0 ± 5.3). Therefore, the E8-SBD123 plants released 12% more glucose units (based on the percentage of hydrolyzed cellulose) than the wild type.

Transgenic plants are more susceptible to digestion than Col-0

Since we observed an alteration in the cell wall composition of the transgenic lines, we investigated the integrity of the cell walls in the transgenic lines and their susceptibility to degradation. Digestibility experiments are valuable for estimating the nutritional value of livestock feed. In the current study, we used two approaches to evaluate the cell wall integrity in the transgenic lines. First, we constructed a dose-response curve using cellulase and macerozyme (Yoo et al. 2007) to obtain protoplasts using the standard protocol (referred to as 1) and different combinations of these enzymes (see "Materials and methods" section), assuming that the number of protoplasts obtained in each case will be proportional to the cell wall digestibility of each plant. As shown in Fig. 5a, the number of protoplasts was significantly higher in both transgenic lines compared to wild type under three of the four conditions analyzed (0.6; 1.0; and 2.0), suggesting that the E8-SBD123 plants are more amenable to digestion than Col-0. Second, we performed a biomass digestibility assay to determine if this behavior would also be observed in an in vivo-like digestion system. In this case, we used an adaptation of a rumen process in

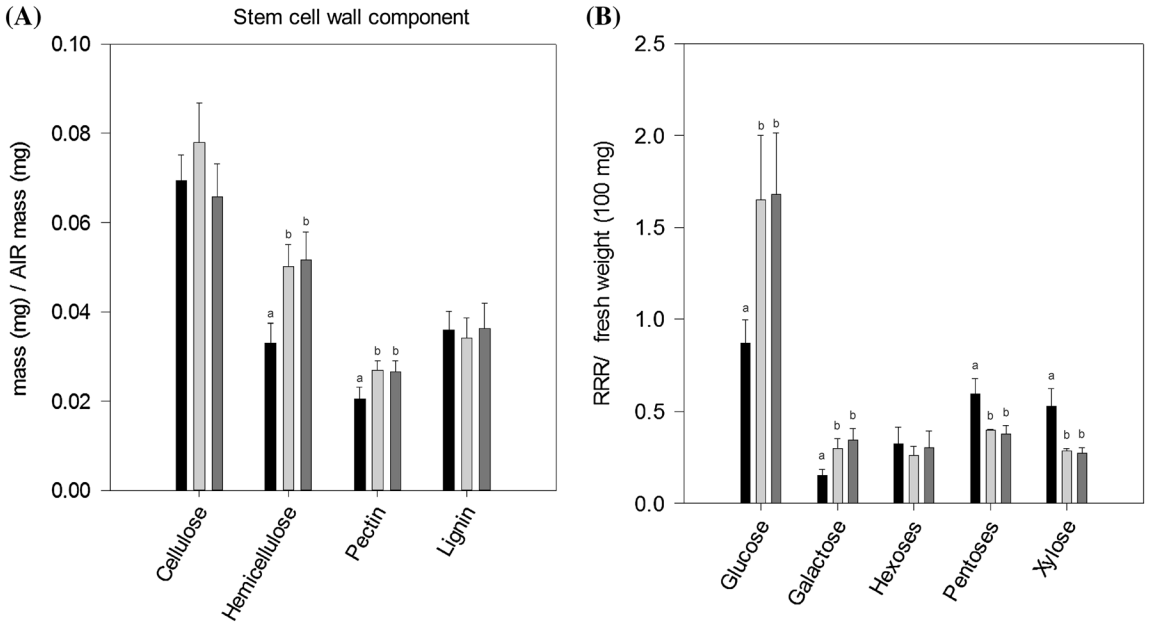

Fig. 4 Cell wall composition in Col-0 and lines E8-SBD123.1 and E8-SBD123.2. **a** Stem cell wall composition analysis of Col-0 (*black*), E8-SBD123.1 (*light gray*) and E8-SBD123.2 (*dark gray*). The data shown are the mean ± SD of three biological replicates. *Lowercase letters* (*a, b*) indicate group or groups that differ from the others using a multiple comparison procedure (Tukey) after statistical analysis with an $\alpha = 0.05$. **b** GCMS sugar profile in hydrolyzed *Arabidopsis thaliana* cell wall extract. The relative response ratio (RRR) is proportional to 100 mg of plant fresh weight. The data represent the mean of four biological replicates. *Significant difference at $p < 0.05$

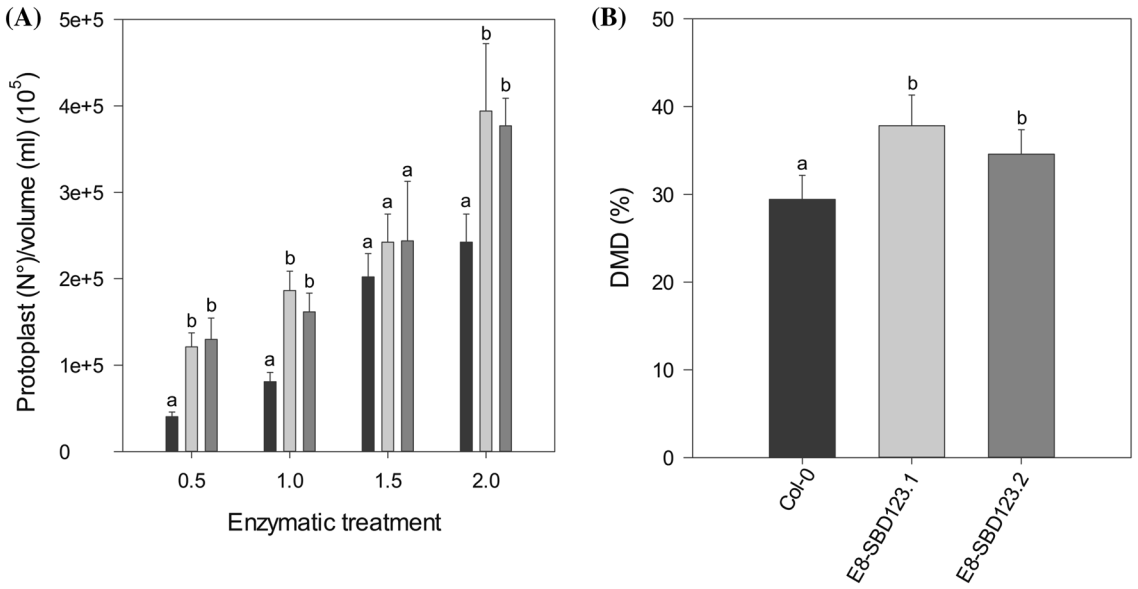

Fig. 5 Cell wall hydrolysis in Col-0 (*black*), E8-SBD123.1 (*light gray*) and E8-SBD123.2 (*dark gray*) lines. **a** Protoplast number obtained by progressive enzymatic treatment and **b** in vitro dry matter digestibility (%) of *Arabidopsis thaliana* plants. *Lowercase letters* (*a* and *b*) indicate group or groups that differ from the others using a multiple comparison procedure (Tukey) within each enzymatic treatment after statistical analysis at $p < 0.05$

an in vitro assay (Tilley and Terry 1963). We found a significant increase (1.28-fold) in DMD in E8-SBD123.1 and a 1.17-fold increase in E8-SBD123.2 (see Fig. 5b) compared to Col-0, suggesting that these plants are more amenable to degradation by external enzymatic processes than Col-0.

Fermentable sugar levels increase as a consequence of the biomass increase

As shown above (Fig. 4b), the amount of carbohydrate released by acid cell wall hydrolysis was higher in the transgenic lines than in wild type. Specifically, there was an increase in glucose and galactose levels and a decrease in xylose levels released after cell wall acid hydrolysis in both transgenic lines compared to wild-type plants. The detection of low amounts of xylose could be because in transgenic plants hemicellulose is more exposed to degradation by increasing the "easy to hydrolyze" fraction (Lavarack et al. 2002), and after hydrolysis, xylose is rapidly degraded to different products, such as furfural (Banerjee et al. 2013).

On the other hand, when total non-hydrolyzed plant extracts were analyzed using an enzymatic approach at three different time points (end of night, midday and end of day), the transgenic and wild-type plants did not differ in terms of fermentable sugars content per fresh weight unit (Supplementary Fig. 5). However, there was an increase in fermentable sugars per plant in the transgenic lines, which was predominantly driven by the increase in biomass ($p < 0.001$; see Supplementary material Fig. 5b, c).

Discussion

Comparative analysis of the adsorption of the SBD123 domain of ATSSIII to polysaccharides indicated that this domain has a degree of promiscuity for binding to different substrates. We analyzed the shapes and composition of the polysaccharide binding sites of enzymes involved in the metabolism of xylanases in the plant cell wall by building an alignment with characterized CBMs to compare their binding sites with existing sites in the starch-binding domains. Using the protein sequences of three CBMs of xylanases from *A. thaliana* (AB008015), *Carica papaya* (AAN10199.1), and *Thermotoga maritima* (AAD35155), which, according to CAZY, are members of the CBM22 family (formerly CBM4_9), we found that the conserved Y394, W340 and W366 residues of SBD123 aligned with residues previously found to participate in xylan binding (Araki et al. 2006; Berrin and Juge 2008; Pollet et al. 2009) (http://www.cazy.org/CBM22_eukaryota.html) (see Supplementary Fig. 6).

In addition, when we analyzed a cellulase endo-(1,4)-β-D-glucanase from *A. thaliana* (At1g64390) involved in cell wall degradation, we found that the cellulose binding domain for this enzyme was also classified in the CBM49 family, which is related to the CBM2 family (http://www.cazy.org/CBM49.html). Three conserved residues (W538, W575 and W589) on the surface of the 3D structure of this protein appear to be responsible for binding to cellulose. The Thr residue W366 of SBD123 aligns with W575, suggesting that it may adsorb to cellulose (Simpson and Barras 1999).

Therefore, in addition to being able to bind to starch, SBD123 also binds to cell wall polysaccharides such as xylan, pectin and cellulose with different affinities, which are even higher than its ability to bind to its natural substrate, starch. The amino acid residues comprising the binding sites (W340, W366 and Y394) with a proven ability to bind to starch, amylose and amylopectin are also involved in binding to xylans, pectins and cellulose.

Based on these results, we investigated the potential use of three *in tandem* SBDs from *A. thaliana* SSIII to obtain transgenic plants with a phenotype of agricultural interest. The E8-SBD123 plants produced in this study had increased biomass due to an increase in cell wall expansion, an altered cell wall composition, lower cell wall integrity and higher amounts of fermentable sugars released after acid hydrolysis compared to wild type. Several attempts have been made to increase plant biomass and to enhance biofuel production through the use of various tools and plant species. Doblin et al. (2014), Kalluri et al. (2014) and Loque et al. (2015) targeted several proteins, including enzymes or transporters involved in nucleotide sugar conversion, enzymes that modify or generate polysaccharides and transcription factors that control the expression of genes encoding key enzymes. Some examples are (i) the overexpression of bacterial hydroxycinnamoyl-CoA hydratase, which improved saccharification and reduced the degree of lignin polymerization in *A. thaliana* (Eudes et al. 2012) and (ii) the overexpression of the Myb transcription factor PvMYB4, which increased ethanol yields from two to sixfold in *Panicum virgatum* (Shen et al. 2013). Another approach involved overexpressing a UDP-galactose transporter to alter cell wall sugar content through manipulating the nucleotide sugar conversion pathway, which increased the hexose/pentose ratio of biomass in *A. thaliana* (Rautengarten et al. 2014). On the other hand, silencing of glycosyltransferase genes involved in xylan biosynthesis (IRX8) in poplar caused a significant reduction in xylan content and increased glucose yields (Biswal et al. 2015). The use of CBMs to modify plant cell walls has also been explored (Levy et al. 2002; Nardi et al. 2015; Obembe et al. 2007; Shoseyov et al. 2001, 2006).

Previous studies have suggested that the presence of the AtSSIII SBD domains could act *in trans*, reestablishing the enzymatic activity of the AtSSIII catalytic domain, in comparison to the full AtSSIII (Wayllace et al. 2010). Thus, we propose that SBDs could act upon cell wall polysaccharides, promoting cellulose creeping and enzymatic attack (Shoseyov et al. 2006). When the cell wall expands, cellulose microfibrils slide between polysaccharide chains using turgor pressure as a driving force until balance against the force of cell wall resistance is achieved. This observation explains why non-hydrolytic "wedge" enzymes favor cellular expansion (Cosgrove 1993; Marga et al. 2005), such as the cellulose binding modules of an exoglucanase (CBM-Cex) from *Cellulomonas fimi*, which can move throughout its substrate's surface (Jervis et al. 1997). A parallel can be drawn between the actions of CBMs expressed in the cell wall and the cell wall-loosening proteins termed expansins (Shoseyov et al. 2006). Moreover, the minimal structure required for the cell wall-loosening activity of Phl p2, an expansin-like protein, is a CBM (Shoseyov et al. 2006). Remarkably, the structure of this CBM, like SBDs, is mainly defined by two binding grooves, which allow the protein to slide between two polysaccharide chains (Southall et al. 1999; Tormo et al. 1996).

Hemicelluloses help strengthen the plant cell wall by interacting with cellulose and, in some walls, lignin (Scheller and Ulvskov 2010). Pectin is involved in numerous physiological processes, such as plant growth and development, defense, cell adhesion and expansion, wall structure and porosity, signaling and pollen tube growth, among others (Mohnen 2008). Therefore, it is thought that the disruption of the cell wall could be mitigated by altering its pectin and hemicellulose contents.

CBMs are thought to play three basic roles with respect to the functioning of their cognate catalytic modules: (i) a proximity effect, (ii) a targeting function and (iii) a disruptive function (Boraston et al. 2004). Thus, the increased biomass degradability phenotype of the E8-SBD123 lines produced in the current study can be attributed to the existence of the putative cell-wall loosening effect of SBD123. However, we cannot exclude the possibility that the activity of any of the degradative enzymes used in this study had differential effects on each plant extract. For example, trans-acting CBMs can modify the activities of several enzymes, such as *A. tumefaciens* glycogen synthase (Martin et al. 2013). In addition, tandem SBDs might behave as scaffolds for the formation of enzyme complexes that remodel the plant cell wall; a scaffolding function has already been demonstrated for starch metabolism enzymes (Hennen-Bierwagen et al. 2009, 2008).

The growing ethanol production industry requires the development of cultivars with high amounts of biomass and low fermentable cell walls. Compounds such as cellulose, pectin and xylan are difficult to degrade, requiring treatment with chemical methods that generate a high number of toxic compounds, which diminished yields during the later stages of fermentation (Nevoigt 2008). In summary, in the current study, we found that purified recombinant SBD123 could bind to cell wall polysaccharides with a higher affinity than to starch. Moreover, when SBD123 was targeted to the cell walls of *A. thaliana* plants, the E8-SBD123 transgenic plants showed an altered cell wall composition and an increase in biomass, which was mainly driven by an increase in cell wall expansion, reduced cell wall integrity, higher levels of cellulose hydrolysis and an increase in fermentable sugars compared to wild type. These results suggest

that the transgenic plants have an advantage for the production of bioethanol in terms of saccharification of essential substrates. In addition, the increased biomass degradability phenotype of E8-SBD123 plants, which may be due to the cell-wall loosening effect of recombinant SBD123, with tandem SBDs, makes such plants promising biotechnological tools for the agricultural and livestock feed industries. However, this strategy must first be tested in a crop of agronomic interest. Further investigations are needed to optimize the desired changes. In addition, an alternative approach to improving the morphological effects throughout the plant would be to employ specific promoters to allow expression of these protein modules only in leaves.

Acknowledgments This work was supported by grants from Agencia Nacional de Promoción Científica y Técnológica (PICT 2010-0543 and PICT 2011-0982), Consejo Nacional de Investigaciones Científicas y Técnicas (CONICET, PIP#237 and #134) and Secretaría de Estado de Ciencia, Tecnología e Innovación de Santa Fe (SECTEI -2010-113-14). MJG and DAP are doctoral fellows from CONICET. HAV, JB, DFGC and MVB are research members from CONICET. The authors thank Ing. Martín Reggiardo-Sobre (CEFOBI) for his technical assistance with the in in vitro dry matter digestibility assays and Bioq. José M. Pellegrino from Instituto de Fisiología Experimental (IFISE) for his advice in general microscopy and image processing.

Author contributions MJG, DAP, JB, DGC, and MVB designed the conception and delineation of the study; prepared the manuscript and reviewed it before submission. MJG, DAP, HAV and JB conducted the required experiments, performed the acquisition of the data or analyzed such information. All authors read and approved the final manuscript.

References

Abbott DW, Boraston AB (2012) Quantitative approaches to the analysis of carbohydrate-binding module function. Methods Enzymol 510:211–231

Abramoff MD, Magelhaes PJ, Ram SJ (2004) Image processing with ImageJ. Biophotonics Int 11:36–42

Araki R, Karita S, Tanaka A, Kimura T, Sakka K (2006) Effect of family 22 carbohydrate-binding module on the thermostability of Xyn10B catalytic module from Clostridium stercorarium. Biosci Biotechnol Biochem 70:3039–3041

Arantes V, Saddler JN (2010) Access to cellulose limits the efficiency of enzymatic hydrolysis: the role of amorphogenesis. Biotechnol Biofuels 3:4

Ball SG, Morell MK (2003) From bacterial glycogen to starch: understanding the biogenesis of the plant starch granule. Annu Rev Plant Biol 54:207–233

Banerjee S, Tayade RA, Sharma BD (2013) Green synthesis of acid esters from furfural via stobbe condensation. J Chem. doi:10.1155/2013/152370

Beemster GT, Baskin TI (1998) Analysis of cell division and elongation underlying the developmental acceleration of root growth in Arabidopsis thaliana. Plant Physiol 116:1515–1526

Bergmeyer H-U (2012) Methods of enzymatic analysis. Elsevier, Amsterdam

Berrin JG, Juge N (2008) Factors affecting xylanase functionality in the degradation of arabinoxylans. Biotechnol Lett 30:1139–1150

Biswal AK, Hao Z, Pattathil S, Yang X, Winkeler K, Collins C, Mohanty SS, Richardson EA, Gelineo-Albersheim I, Hunt K, Ryno D, Sykes RW, Turner GB, Ziebell A, Gjersing E, Lukowitz W, Davis MF, Decker SR, Hahn MG, Mohnen D (2015) Down-regulation of GAUT12 in Populus deltoides by RNA silencing results in reduced recalcitrance, increased growth and reduced xylan and pectin in a woody biofuel feedstock. Biotechnol Biofuels 8:41

Blumenkrantz N, Asboe-Hansen G (1973) New method for quantitative determination of uronic acids. Anal Biochem 54:484–489

Bolam DN, Ciruela A, McQueen-Mason S, Simpson P, Williamson MP, Rixon JE, Boraston A, Hazlewood GP, Gilbert HJ (1998) Pseudomonas cellulose-binding domains mediate their effects by increasing enzyme substrate proximity. Biochem J 331(Pt 3):775–781

Boraston AB, Bolam DN, Gilbert HJ, Davies GJ (2004) Carbohydrate-binding modules: fine-tuning polysaccharide recognition. Biochem J 382:769–781

Boyes DC, Zayed AM, Ascenzi R, McCaskill AJ, Hoffman NE, Davis KR, Gorlach J (2001) Growth stage-based phenotypic analysis of Arabidopsis: a model for high throughput functional genomics in plants. Plant Cell 13:1499–1510

Buleon A, Colonna P, Planchot V, Ball S (1998) Starch granules: structure and biosynthesis. Int J Biol Macromol 23:85–112

Busi MV, Palopoli N, Valdez HA, Fornasari MS, Wayllace NZ, Gomez-Casati DF, Parisi G, Ugalde RA (2008) Functional and structural characterization of the catalytic domain of the starch synthase III from *Arabidopsis thaliana*. Proteins 70:31–40

Busi M, Gomez-Casati D, Martín M, Barchiesi J, Grisolía M, Hedín N, Carrillo J (2014) Starch metabolism in green plants. In: Ramawat KG, Mérillon J-M (eds) Polysaccharides. Springer, New York, pp 1–42

Cantarel BL, Coutinho PM, Rancurel C, Bernard T, Lombard V, Henrissat B (2009) The Carbohydrate-Active EnZymes database (CAZy): an expert resource for Glycogenomics. Nucleic Acids Res 37:D233–D238

Carpita NC (1996) Structure and biogenesis of the cell walls of grasses. Annu Rev Plant Physiol Plant Mol Biol 47:445–476

Cassab GI (1998) Plant cell wall proteins. Annu Rev Plant Physiol Plant Mol Biol 49:281–309

Clough SJ, Bent AF (1998) Floral dip: a simplified method for Agrobacterium-mediated transformation of Arabidopsis thaliana. Plant J 16:735–743

Cosgrove DJ (1993) How do plant cell walls extend? Plant Physiol 102:1–6

d'Amour J, Gosselin C, Arul J, Castaigne F, Willemot C (1993) Gamma-radiation affects cell wall composition of strawberries. J Food Sci 58:182–185

Denyer K, Sidebottom C, Hylton CM, Smith AM (1993) Soluble isoforms of starch synthase and starch-branching enzyme also occur within starch granules in developing pea embryos. Plant J 4:191–198

Doblin MS, Johnson KL, Humphries J, Newbigin EJ, Bacic A (2014) Are designer plant cell walls a realistic aspiration or will the plasticity of the plant's metabolism win out? Curr Opin Biotechnol 26:108–114

Donnelly PM, Bonetta D, Tsukaya H, Dengler RE, Dengler NG (1999) Cell cycling and cell enlargement in developing leaves of Arabidopsis. Dev Biol 215(407 –):19

Duryea ML (1985) Evaluating seedling quality: principles, procedures, and predictive abilities of major tests. In: Proceedings of the workshop held October 16–18, 1984

Eudes A, George A, Mukerjee P, Kim JS, Pollet B, Benke PI, Yang F, Mitra P, Sun L, Cetinkol OP, Chabout S, Mouille G, Soubigou-Taconnat L, Balzergue S, Singh S, Holmes BM, Mukhopadhyay A, Keasling JD, Simmons BA, Lapierre C, Ralph J, Loque D

(2012) Biosynthesis and incorporation of side-chain-truncated lignin monomers to reduce lignin polymerization and enhance saccharification. Plant Biotechnol J 10:609–620

Gomez-Casati DF, Martin M, Busi MV (2013) Polysaccharide-synthesizing glycosyltransferases and carbohydrate binding modules: the case of starch synthase III. Protein Pept Lett 20:856–863

Hatfield RD, Grabber J, Ralph J, Brei K (1999) Using the acetyl bromide assay to determine lignin concentrations in herbaceous plants: some cautionary notes. J Agric Food Chem 47:628–632

Hennen-Bierwagen TA, Liu F, Marsh RS, Kim S, Gan Q, Tetlow IJ, Emes MJ, James MG, Myers AM (2008) Starch biosynthetic enzymes from developing maize endosperm associate in multisubunit complexes. Plant Physiol 146:1892–1908

Hennen-Bierwagen TA, Lin Q, Grimaud F, Planchot V, Keeling PL, James MG, Myers AM (2009) Proteins from multiple metabolic pathways associate with starch biosynthetic enzymes in high molecular weight complexes: a model for regulation of carbon allocation in maize amyloplasts. Plant Physiol 149:1541–1559

Hoebler C, Barry JL, David A, Delort-Laval J (1989) Rapid acid hydrolysis of plant cell wall polysaccharides and simplified quantitative determination of their neutral monosaccharides by gas-liquid chromatography. J Agric Food Chem 37:360–367

Horiguchi G, Kim GT, Tsukaya H (2005) The transcription factor AtGRF5 and the transcription coactivator AN3 regulate cell proliferation in leaf primordia of *Arabidopsis thaliana*. Plant J 43:68–78

Iiyama K, Wallis AFA (1988) An improved acetyl bromide procedure for determining lignin in Woods and wood pulps. Wood Sci Technol 22:271–280

James MG, Denyer K, Myers AM (2003) Starch synthesis in the cereal endosperm. Curr Opin Plant Biol 6:215–222

Jervis EJ, Haynes CA, Kilburn DG (1997) Surface diffusion of cellulases and their isolated binding domains on cellulose. J Biol Chem 272:24016–24023

Kalluri UC, Yin H, Yang X, Davison BH (2014) Systems and synthetic biology approaches to alter plant cell walls and reduce biomass recalcitrance. Plant Biotechnol J 12:1207–1216

Koornneef M, Hanhart CJ, van der Veen JH (1991) A genetic and physiological analysis of late flowering mutants in *Arabidopsis thaliana*. Mol Gen Genet 229:57–66

Kopka J, Schauer N, Krueger S, Birkemeyer C, Usadel B, Bergmuller E, Dormann P, Weckwerth W, Gibon Y, Stitt M, Willmitzer L, Fernie AR, Steinhauser D (2005) GMD@CSB.DB: the Golm metabolome database. Bioinformatics 21:1635–1638

Larran A, Jozami E, Vicario L, Feldman SR, Podesta FE, Permingeat HR (2015) Evaluation of biological pretreatments to increase the efficiency of the saccharification process using Spartina argentinensis as a biomass resource. Bioresour Technol 194:320–325

Lavarack BP, Griffin GJ, Rodman D (2002) The acid hydrolysis of sugarcane bagasse hemicellulose to produce xylose, arabinose, glucose and other products. Biomass Bioenergy 23:367–380

Levy I, Shani Z, Shoseyov O (2002) Modification of polysaccharides and plant cell wall by endo-1, 4-β-glucanase and cellulose-binding domains. Biomol Eng 19:14

Lisec J, Schauer N, Kopka J, Willmitzer L, Fernie AR (2006) Gas chromatography mass spectrometry-based metabolite profiling in plants. Nat Protoc 1:387–396

Loque D, Scheller HV, Pauly M (2015) Engineering of plant cell walls for enhanced biofuel production. Curr Opin Plant Biol 25:151–161

Marga F, Grandbois M, Cosgrove DJ, Baskin TI (2005) Cell wall extension results in the coordinate separation of parallel microfibrils: evidence from scanning electron microscopy and atomic force microscopy. Plant J 43:181–190

Martin M, Wayllace NZ, Valdez HA, Gomez-Casati DF, Busi MV (2013) Improving the glycosyltransferase activity of *Agrobacterium tumefaciens* glycogen synthase by fusion of N-terminal starch binding domains (SBDs). Biochimie 95:1865–1870

Minic Z, Jamet E, San-Clemente H, Pelletier S, Renou JP, Rihouey C, Okinyo DP, Proux C, Lerouge P, Jouanin L (2009) Transcriptomic analysis of Arabidopsis developing stems: a close-up on cell wall genes. BMC Plant Biol 9:6

Mohnen D (2008) Pectin structure and biosynthesis. Curr Opin Plant Biol 11:266–277

Nardi CF, Villarreal NM, Rossi FR, Martinez S, Martinez GA, Civello PM (2015) Overexpression of the carbohydrate binding module of strawberry expansin2 in *Arabidopsis thaliana* modifies plant growth and cell wall metabolism. Plant Mol Biol 88:101–117

Nevoigt E (2008) Progress in metabolic engineering of *Saccharomyces cerevisiae*. Microbiol Mol Biol Rev 72:379–412

Obembe OO, Jacobsen E, Visser R, Vincken JP (2007) Expression of an expansin carbohydrate-binding module affects xylem and phloem formation. Afr J Biotechnol 6:9

Palopoli N, Busi MV, Fornasari MS, Gomez-Casati D, Ugalde R, Parisi G (2006) Starch-synthase III family encodes a tandem of three starch-binding domains. Proteins 65:27–31

Pollet A, Sansen S, Raedschelders G, Gebruers K, Rabijns A, Delcour JA, Courtin CM (2009) Identification of structural determinants for inhibition strength and specificity of wheat xylanase inhibitors TAXI-IA and TAXI-IIA. FEBS J 276:3916–3927

Rautengarten C, Ebert B, Moreno I, Temple H, Herter T, Link B, Donas-Cofre D, Moreno A, Saez-Aguayo S, Blanco F, Mortimer JC, Schultink A, Reiter WD, Dupree P, Pauly M, Heazlewood JL, Scheller HV, Orellana A (2014) The Golgi localized bifunctional UDP-rhamnose/UDP-galactose transporter family of Arabidopsis. Proc Natl Acad Sci USA 111:11563–11568

Ritchie GA (1984) Assesing seedling quality. In: Duryea ML, Landis TD (eds) Forest nursery manual: production of bareroot seedlings. Martinus Nijhoff/Dr W. Junk Publishers, The Hague/Boston/Lancaster, pp 243–259

Rodriguez RE, Mecchia MA, Debernardi JM, Schommer C, Weigel D, Palatnik JF (2010) Control of cell proliferation in *Arabidopsis thaliana* by microRNA miR396. Development 137:103–112

Rodriguez-Sanoja R, Ruiz B, Guyot JP, Sanchez S (2005) Starch-binding domain affects catalysis in two Lactobacillus alpha-amylases. Appl Environ Microbiol 71:297–302

Rohila JS, Chen M, Cerny R, Fromm ME (2004) Improved tandem affinity purification tag and methods for isolation of protein heterocomplexes from plants. Plant J 38:172–181

Rymen B, Coppens F, Dhondt S, Fiorani F, Beemster GT (2010) Kinematic analysis of cell division and expansion. Methods Mol Biol 655:203–227

Sato K, Suzuki R, Nishikubo N, Takenouchi S, Ito S, Nakano Y, Nakaba S, Sano Y, Funada R, Kajita S, Kitano H, Katayama Y (2010) Isolation of a novel cell wall architecture mutant of rice with defective Arabidopsis COBL4 ortholog BC1 required for regulated deposition of secondary cell wall components. Planta 232:257–270

Scheller HV, Ulvskov P (2010) Hemicelluloses. Annu Rev Plant Biol 61:263–289

Shen H, Poovaiah CR, Ziebell A, Tschaplinski TJ, Pattathil S, Gjersing E, Engle NL, Katahira R, Pu Y, Sykes R, Chen F, Ragauskas AJ, Mielenz JR, Hahn MG, Davis M, Stewart CN, Jr., Dixon RA (2013) Enhanced characteristics of genetically modified switchgrass (*Panicum virgatum* L.) for high biofuel production. Biotechnol Biofuels 6: 71

Shoseyov O, Shani Z, Shpigel E (2001) Transgenic plants of altered morphology. US Patent 6,184,440. US Patent and Trademark Office, Washington DC

Shoseyov O, Shani Z, Levy I (2006) Carbohydrate binding modules: biochemical properties and novel applications. Microbiol Mol Biol Rev 70(283 –):95

Simpson HD, Barras F (1999) Functional analysis of the carbohydrate-binding domains of Erwinia chrysanthemi Cel5 (Endoglucanase Z) and an Escherichia coli putative chitinase. J Bacteriol 181:4611–4616

Southall SM, Simpson PJ, Gilbert HJ, Williamson G, Williamson MP (1999) The starch-binding domain from glucoamylase disrupts the structure of starch. FEBS Lett 447:58–60

Teeri TT, Penttila M, Keranen S, Nevalainen H, Knowles JK (1992) Structure, function, and genetics of cellulases. Biotechnology 21:417–445

Tetlow IJ, Morell MK, Emes MJ (2004) Recent developments in understanding the regulation of starch metabolism in higher plants. J Exp Bot 55:2131–2145

Tilley JMA, Terry RA (1963) A two-stage technique for the in vitro digestion of forage crops. Grass Forage Sci 18:104–111

Tormo J, Lamed R, Chirino AJ, Morag E, Bayer EA, Shoham Y, Steitz TA (1996) Crystal structure of a bacterial family-III cellulose-binding domain: a general mechanism for attachment to cellulose. EMBO J 15:5739–5751

Turner SR, Somerville CR (1997) Collapsed xylem phenotype of Arabidopsis identifies mutants deficient in cellulose deposition in the secondary cell wall. Plant Cell 9:689–701

Valdez HA, Busi MV, Wayllace NZ, Parisi G, Ugalde RA, Gomez-Casati DF (2008) Role of the N-terminal starch-binding domains in the kinetic properties of starch synthase III from *Arabidopsis thaliana*. Biochemistry 47:3026–3032

Valdez HA, Peralta DA, Wayllace NZ, Grisolía MJ, Gomez-Casati DF, Busi MV (2011) Preferential binding of SBD from Arabidopsis thaliana SSIII to polysaccharides: Study of amino acid residues involved. Starch/Stärke 63:451–460

Vicente AR, Costa ML, Martínez GA, Chaves AR, Civello PM (2005) Effect of heat treatments on cell wall degradation and softening in strawberry fruit. Postharvest Biol Technol 38:213–222

Wayllace NZ, Valdez HA, Ugalde RA, Busi MV, Gomez-Casati DF (2010) The starch-binding capacity of the noncatalytic SBD2 region and the interaction between the N- and C-terminal domains are involved in the modulation of the activity of starch synthase III from *Arabidopsis thaliana*. FEBS J 277:428–440

Weigel D, Glazebrook J (2002) A laboratory manual. CSHL Press, pp 1–354

Willats WG, Orfila C, Limberg G, Buchholt HC, van Alebeek GJ, Voragen AG, Marcus SE, Christensen TM, Mikkelsen JD, Murray BS, Knox JP (2001) Modulation of the degree and pattern of methyl-esterification of pectic homogalacturonan in plant cell walls. Implications for pectin methyl esterase action, matrix properties, and cell adhesion. J Biol Chem 276:19404–19413

Ye J, Coulouris G, Zaretskaya I, Cutcutache I, Rozen S, Madden TL (2012) Primer-BLAST: a tool to design target-specific primers for polymerase chain reaction. BMC Bioinformatics 13:134

Yoo SD, Cho YH, Sheen J (2007) Arabidopsis mesophyll protoplasts: a versatile cell system for transient gene expression analysis. Nat Protoc 2:1565–1572

Zhang X, Szydlowski N, Delvalle D, D'Hulst C, James MG, Myers AM (2008) Overlapping functions of the starch synthases SSII and SSIII in amylopectin biosynthesis in Arabidopsis. BMC Plant Biol 8:96